

# A SIMULATION STUDY ON POINT DETERMINATION FOR THE MOMS-02/D2 SPACE PROJECT USING AN EXTENDED FUNCTIONAL MODEL

H. Ebner, W. Kornus, T. Ohlhof

Chair for Photogrammetry and Remote Sensing  
Technical University Munich  
Arcisstr. 21, D-8000 Munich 2, Germany  
Tel: + 49-89-2105 2671; Fax: + 49-89-280 95 73; Telex: 522854 tumue d  
E-mail: ebner@photo.verm.tu-muenchen.de

Commission IV

## ABSTRACT:

In the course of the 2nd German Spacelab mission D2, scheduled for launch in 1993, the MOMS-02 camera is intended to acquire digital threefold stereo imagery of the earth's surface from space. In former simulations the influence of certain mission parameters on the attainable geometric accuracy has already been examined. With regard to the future compilation of real data, the functional model was extended with respect to the special MOMS-02 camera geometry and the actual orbit.

After a brief description of the extended model, the results of new simulations are presented. They show the influence of the precision of observed exterior orientation parameters, the type and density of ground control, the camera inclination across flight direction and the simultaneous adjustment of two crossing strips with different intersection angles on the theoretical accuracy of the point determination. Because of the improved functional model the obtained accuracy estimates are expected to be representative for the practical project. Finally conclusions are drawn from these results.

**KEY WORDS:** Accuracy, Aerotriangulation, Space Imagery, 3-D.

## 1. INTRODUCTION

MOMS-02/D2 is a digital camera project in the framework of the second German Spacelab mission D2 scheduled to be launched in early 1993. The optical system of the MOMS-02 camera consists of a stereo module with three panchromatic channels and a multispectral module with four colour channels. The stereo data acquisition will be performed by three linear arrays of CCD detectors.

From the photogrammetric point of view the scientific objectives of the mission are (Ackermann et al., 1990):

- ▶ the generation of a Digital Terrain Model (DTM) with a standard deviation of 5 m,
- ▶ the production of high quality topographic and orthoimage maps and
- ▶ the development of a softcopy (digital) photogrammetric workstation.

With respect to the digital nature of the primary information, the data processing of three-line-camera imagery has to be performed completely in the digital domain. The concept for a fully digital photogrammetric data acquisition and evaluation is shown in (Heipke et al., 1990).

Within the MOMS-02/D2 science team the Chair for Photogrammetry and Remote Sensing of the Technical University Munich is responsible for the threedimensional point determination by bundle adjustment including the reconstruction of the exterior orientation. The functional model was adopted step by step according to the geometric specifications of the mission. The latest extensions are

described in detail. Results of computer simulations using the extended model are presented, which verify the theoretical accuracy. Finally, conclusions are drawn and recommendations for future line camera missions are given.

## 2. EXTENSION OF THE FUNCTIONAL MODEL

The forthcoming evaluation of practical MOMS-02 imagery is to be carried out using the bundle block adjustment program CLIC, developed at the Chair for Photogrammetry and Remote Sensing (TU Munich, 1992). The functional model of CLIC has to be adopted according to the geometric specifications of the MOMS-02/D2 project. The most important extensions, concerning the camera geometry, the reconstruction of the exterior orientation and the introduction of offset and drift parameters are described in the following.

### 2.1 Camera geometry

The 3 lenses of the MOMS-02 stereo module provide a threefold along track stereo scanning with different ground resolutions. The focal length  $c_N$  of the nadir (N) looking high resolution (HR) lens amounts to 660.0 mm, the forward (F) and backward (B) looking lenses are inclined with respect to the HR lens by  $\pm 21.9^\circ$  and have a focal length of 237.2 mm each ( $c_F, c_B$ ).

Figure 1 schematically shows the optical system of the MOMS-02 camera. The inclined stereo lenses are represen-

ted in the foreground. Behind, the HR lens is visible, arranged between two additional lenses for multispectral data acquisition.

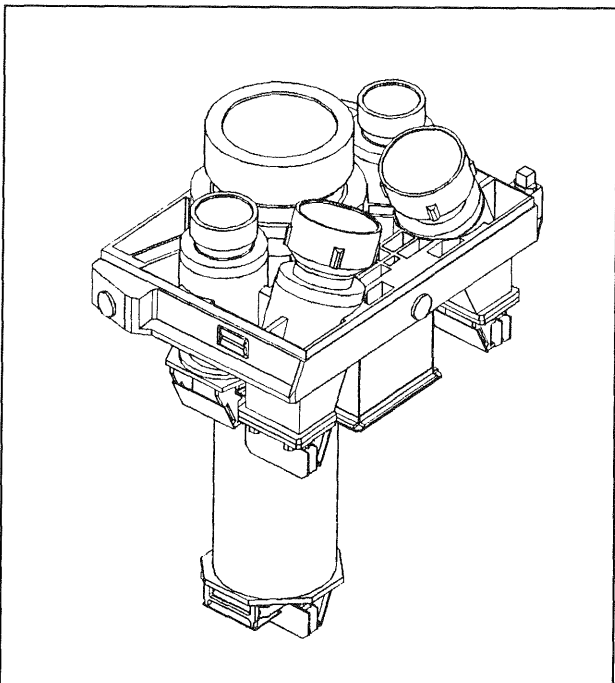


Fig. 1: Optical system of MOMS-02

For the illustration of the functional model, the object coordinate system  $XYZ$  and the image coordinate systems of the HR lens  $x_N, y_N, z_N$  and the forward looking lens  $x_F, y_F, z_F$  are represented in Figure 2. All coordinate systems are right handed Cartesian, at which the image coordinate systems are defined as follows:

- ▶ origin: centre of the first active pixel of the sensor line,
- ▶ direction of z-axis: parallel to the optical axis, pointing downward,
- ▶ direction of y-axis: straight line through all pixel centres,
- ▶ direction of x-axis: orthogonally completed, close to direction of flight.

For each inclined lens an additional 6 parameter transformation was introduced to rigorously model the displacements  $\Delta x, \Delta y, \Delta z$  of the projection centres (PC) and the rotations  $\Delta \varphi, \Delta \omega, \Delta \kappa$  of the image coordinate system with respect to the image coordinate system of the HR lens. Thus, the MOMS-02 camera geometry is described by 21 parameters: 2 x 9 parameters ( $\Delta \varphi_{FB}, \Delta \omega_{FB}, \Delta \kappa_{FB}, \Delta x_{FB}, \Delta y_{FB}, \Delta z_{FB}, x_{OF,FB}, y_{OF,FB}, c_{FB}$ ) for the forward and the backward (FB) looking lens each, and 3 parameters ( $x_{ON}, y_{ON}, c_N$ ) for the nadir looking lens. In principle, these parameters can simultaneously be estimated by the bundle adjustment. In practice they will be treated as constant values, determined by camera calibration previously. The extended collinearity equations (2) are derived from the general approach (1) and are applied for the inclined lenses. In case of the nadir looking lens ( $\Delta x_N = \Delta y_N = \Delta z_N = 0, M = I$ ) the classical collinearity equations are obtained from (2).

- $x, y$  : image coordinates of the object point
- $x_0, y_0$  : image coordinates of the principal point
- $k$  : scale factor
- $M, D, R$  : rotation matrices ( $M^T D^T = R^T$ )
- $X, Y, Z$  : ground coordinates of the object point

- $X_0, Y_0, Z_0$  : ground coordinates of the projection centre of the nadir looking HR lens (position)
- $\varphi_0, \omega_0, \kappa_0$  : rotation angles of exterior orientation of the nadir looking HR lens (attitude)

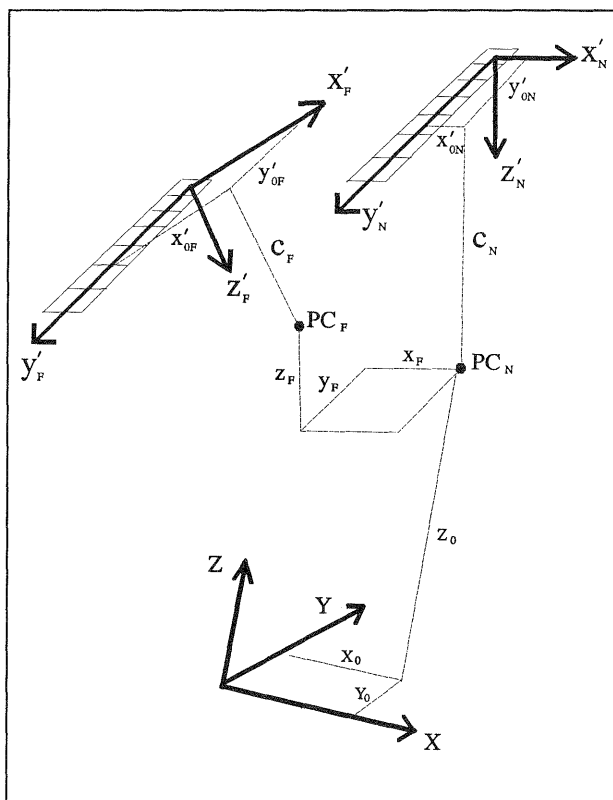


Fig. 2: Coordinate systems

$$\begin{pmatrix} x - x_0 \\ y - y_0 \\ -c \end{pmatrix} = k M^T(\Delta \varphi, \Delta \omega, \Delta \kappa) D^T(\varphi_0, \omega_0, \kappa_0) \begin{pmatrix} X - (X_0 + \Delta X_0) \\ Y - (Y_0 + \Delta Y_0) \\ Z - (Z_0 + \Delta Z_0) \end{pmatrix}$$

$$\text{with } \begin{pmatrix} \Delta X_0 \\ \Delta Y_0 \\ \Delta Z_0 \end{pmatrix} = D(\varphi_0, \omega_0, \kappa_0) \begin{pmatrix} \Delta x \\ \Delta y \\ \Delta z \end{pmatrix} \quad (1)$$

$$\begin{aligned} x &= x_0 - c \frac{R_{11}(X - X_0) + R_{21}(Y - Y_0) + R_{31}(Z - Z_0) - [M_{11}\Delta x + M_{21}\Delta y + M_{31}\Delta z]}{R_{13}(X - X_0) + R_{23}(Y - Y_0) + R_{33}(Z - Z_0) - [M_{13}\Delta x + M_{23}\Delta y + M_{33}\Delta z]} \\ y &= y_0 - c \frac{R_{12}(X - X_0) + R_{22}(Y - Y_0) + R_{32}(Z - Z_0) - [M_{12}\Delta x + M_{22}\Delta y + M_{32}\Delta z]}{R_{13}(X - X_0) + R_{23}(Y - Y_0) + R_{33}(Z - Z_0) - [M_{13}\Delta x + M_{23}\Delta y + M_{33}\Delta z]} \end{aligned} \quad (2)$$

This general approach allows for processing randomly orientated image coordinate systems of lenses with different interior orientations ( $x_0, y_0, c$ ). Self-calibration using additional parameters for the correction of systematic image errors can be applied as usual.

To demonstrate the influence of different focal lengths  $c_N$  and  $c_{FB}$ , the standard deviations  $\sigma_x, \sigma_y, \sigma_z$  of a symmetrical 3-ray forward intersection (standard deviations of image coordinates  $\sigma_0$ , flying height  $h$ , baselength  $b, \varphi_0 = \omega_0 = \kappa_0 = 0$ ) are listed (3). It is conspicuous, that the height accuracy does not depend on  $c_N$ , whereas all 3 rays contribute to the planimetric accuracy. The MOMS-02 geometry ( $c_N : c_{FB} = 3:1$ ) improves the accuracy in planimetry by a factor of

about 2 compared to the ratio of 1:1. The height accuracy is not affected, as mentioned already.

$$\sigma_x = \sigma_y = \sigma_0 h \sqrt{\frac{1}{2c_{F,B}^2 + c_N^2}}; \quad \sigma_z = \sigma_0 \frac{h^2}{b} \sqrt{\frac{1}{2c_{F,B}^2}} \quad (3)$$

## 2.2 Reconstruction of the exterior orientation

The functional model of the bundle adjustment is based on extended collinearity equations. The exterior orientation parameters are estimated only for so-called orientation images (OI), which are introduced at certain time intervals. Between the OI, the parameters of each individual image line are expressed as functions (e.g. polynomials) of the parameters of the neighbouring orientation images (Müller, 1991). A variety of different parameter models for the reconstruction of the exterior orientation were applied in the past (see survey in Wu, 1986). The goal of each approach is the minimization of the interpolation error using as few parameters as possible.

Investigations, based on simulated orbit data, showed that 3rd order polynomial functions approximate the orbit quite accurately. Therefore the linear interpolation function, used in the bundle block adjustment program CLIC previously, was replaced by a Lagrange Polynomial (LP) approach (4).

$$P_n(t) = \sum_{i=0}^n P(t_i) \prod_{\substack{j=0 \\ j \neq i}}^n \frac{t - t_j}{t_i - t_j} \quad (4)$$

In (4) the exterior orientation parameters  $P_n(t)$  at time  $t$  are expressed as a linear combination of the related parameters  $P(t_i)$  assigned to the  $n+1$  neighbouring orientation images  $i$  at time  $t_i$ . The main characteristics of the LPs are: The LP coefficients are explicitly the (unknown) exterior orientation parameters of the orientation images; the LP order can easily be changed by the definition of the parameter  $n$ . The linear interpolation therefore remains applicable by setting  $n = 1$ . The complete extended collinearity equations are derived by replacing the exterior orientation elements  $X_0$ ,  $Y_0$ ,  $Z_0$ ,  $\varphi_0$ ,  $\omega_0$ ,  $\kappa_0$  in equations (2) by the related expressions (4).

## 2.3 Introduction of offset and drift parameters

In principle, the reconstruction of the exterior orientation of three-line-imagery is possible by means of photogrammetric measurements and ground control information only. However, precise position and attitude observations essentially improve the accuracy of point determination, especially if little or weak ground control information is available (Ebner et al., 1991).

In case of MOMS-02/D2, the following additional information is available:

- ▶ position and attitude data from an onboard Inertial Navigation System (INS),
- ▶ position data from the Tracking Data Relay Satellite System (TDRSS),
- ▶ position data from sophisticated orbit models.

All these rather heterogeneous data of position and attitude have to be combined and transformed into a common coordinate system.

Basically, all measurements are affected by blunders, random and systematic errors. Blunders must be located and eliminated a priori by robust estimation methods. Random errors can be processed by least squares adjustment. The critical aspect is the influence of systematic errors. They should be described by the functional model.

In our case the different systematic errors of the position and attitude data are modeled through additional unknown parameters. By limitation to constant and linear terms which, describe the main effects, twelve additional parameters, namely an offset and a drift parameter for each exterior orientation parameter, have to be estimated during the bundle adjustment.

## 3. SIMULATIONS

In the past a series of simulations was carried out for MOMS-02/D2 to analyze the effect of certain parameters on the accuracy of point determination and to give recommendations in the planning phase of the project concerning the technical design of the camera or additional measurements during the mission (Ebner et al., 1991; Ebner and Kornus, 1991). Based on these results, new simulations are performed to show the attainable accuracy using the extended functional model and realistic input information. In the following the input information and the results of the simulations are presented.

### 3.1 Input information

**3.1.1 Camera and mission parameters** The geometric configuration is established by the MOMS-02/D2 camera and mission specifications. The most conspicuous feature is the extremely small image angle, which results in a ratio between flying height and swath width of 8:1. This is an essential handicap for a precise geometric evaluation. The parameters used in the simulations are listed in table 1 and match the nominal values of the project to a large extent.

view direction of the lens	forward	nadir	backward
calibrated focal length [mm]	237.2	660.0	237.2
pixel size [ $\mu$ m]	10.0	10.0	10.0
ground resolution [m]	13.5	4.5	13.5
convergency angle $\Delta\varphi$ [deg]	-21.9	0.0	21.9
orbit height [km]	296		
orbit inclination [deg]	28.5		
swath width [km]	36		
strip length [km]	468		

Table 1: Simulation parameters

The camera is mounted on top of the space shuttle, which will move along a 296 km high orbit with an inclination of 28.5°. Besides the recording of single strips in normal (bay down) flight attitude of the shuttle, some orbits will be flown with a shuttle cross inclination of 30°. As shown in (Ebner et al., 1991) the accuracy of point determination can be improved by convergent sensor configuration either obtained by an instrumental sensor line convergency or by inclining the camera carrier in case of parallel sensor arrangement.

By the simultaneous adjustment of two crossing strips recorded from two different orbits further improvement can be achieved, especially in the common area covered by both strips. Intersection angles of ground tracks of two orbits can range from very small angles at 28.5° northern or southern latitude up to 57° at the equator. Simulations have been performed using the three intersection angles 5°, 30° and 55°.

All points located within the first or the last baselength of a strip are imaged by two sensors only (2-ray points). Within the overlapping area of two crossing strips the points can be projected into a maximum of six sensor lines (6-ray points). Figure 3 shows the different numbers of possible image rays, contributing to the determination of the corresponding object point.

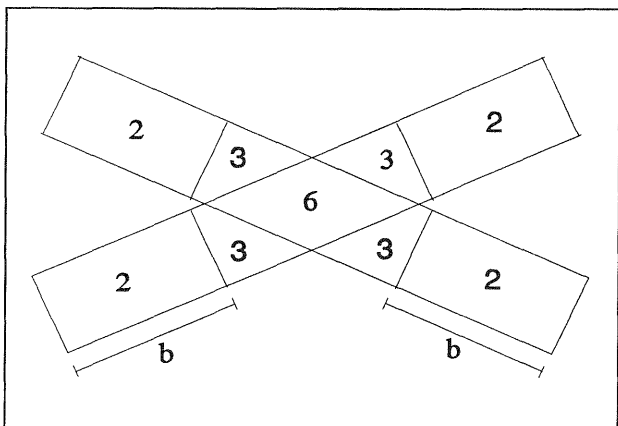


Fig. 3: Numbers of possible image rays, contributing to the point determination

**3.1.2 Image coordinates of conjugate points and ground control points (GCP)** The digitally recorded MOMS-02 imagery will be available on computer compatible tapes (CCT) and thus will directly be accessible for the further digital processing. After radiometric correction a large number of image coordinates of conjugate points can automatically be derived by digital image matching techniques. Involving least squares adjustment a precision up to 1/10 of the pixel size can be achieved. How far the three times higher ground resolution of the HR channel additionally improves the accuracy has still to be investigated.

The determination of image coordinates of GCP implies the identification of the points in the image. Up to now this task must be carried out interactively using e. g. a softcopy photogrammetric workstation.

For the simulations the image coordinates of 11905 object points with a constant height of 0.0 m were computed, assuming a straight forward flight path ( $\varphi_0 = \omega_0 = \kappa_0 = 0^\circ$ ). The points are arranged in a grid within an 36 x 468 km<sup>2</sup> area. The distance between two points is chosen to be 9 km across track and 0.2 km along track. The x-axis of the object coordinate system is defined parallel to the direction of flight. All image coordinates were introduced into the adjustment as uncorrelated observations with equal standard deviations of 2 μm (1/5 pixel size).

**3.1.3 Ground control information** In principle, ground control information is necessary to define the datum, i.e. for positioning, orientation and scale of the photogrammetric

model in a selected reference frame, and to improve the accuracy of the point determination. Due to the low orbital inclination only regions close to the equator can be imaged by the MOMS-02 camera. In most of these countries the number and accuracy of GCP is rather limited.

In the simulations two kinds of control information are used:

- ▶ 4 XYZ GCP, error-free;
- ▶ 125 XY GCP and a Digital Terrain Model (DTM) with standard deviations of 25 m (GCP) and 50 m (DTM), respectively.

In the first case, the four XYZ GCP are arranged at the corners of the 3-ray area. Their coordinates are treated as error-free. By means of measurements with the Global Positioning System (GPS), that is available all over the world, it is possible to determine these GCP economically at an accuracy level of a few centimetres.

In the second case, a lot of XY GCP and a DTM, which might be derived from existing maps via digitization, are employed. From topographic maps in the scale of 1:50.000 characteristic points, e. g. cross-roads, can be digitized with a planimetric accuracy of about 20 to 30 m. The generation of DTM using contour lines is presented in (Aumann and Ebner, 1992); from the mentioned topographic maps 1:50.000 a height accuracy of at least 50 m can be achieved. The mathematical model for using DTM information in a bundle block adjustment is described in (Ebner and Strunz, 1988).

### 3.1.4 Observations of the exterior orientation parameters

The derived position and attitude data from navigation systems and orbit models, mentioned in chapter 2.3, are introduced with the following standard deviations:

position parameters	attitude parameters
▶ 0 m (error-free)	0 mgrad (error-free)
▶ 1 m	5 mgrad
▶ 2 m	10 mgrad
▶ ∞ (no observation)	∞ (no observation)

According to the current knowledge the position data can be obtained more precisely than the attitude data. For instance, an attitude accuracy of 5 mgrad is equivalent to a position accuracy of 25 m considering the orbit height of 296 km. In our case, an accuracy of about 1 to 2 m for the position and 5 to 10 mgrad for the attitude is expected. In addition, the two extreme cases - error-free and no observations - are applied comparatively.

Furthermore, the observed position and attitude data have low absolute but high relative accuracy with respect to the reference coordinate system because of unknown systematic errors, which are modeled by the twelve offset and drift parameters as described in chapter 2.3.

### 3.1.5 Distances between the orientation images (DOI)

The suitable DOI has to be adapted to the temporal variations of the position and attitude of the shuttle. The aim is to derive such a DOI, that the exterior orientation parameters are optimally approximated by a mathematical model, i.e. a 3rd order Lagrange polynomial in this case. It must be considered that a long distance between the orientation images leads to interpolation errors and deteriorates the accuracy. In future, the program CLIC

should be able to use different DOI for the position and the attitude orientation parameters.

The simulations were carried out using the following values:

	DOI	flight time	number of OI
▶	12 km	1.7 sec	40
▶	23 km	3.2 sec	20
▶	160 km	22.5 sec	4

### 3.2 Results

In order to present the results of the different computation versions in a compact form the root-mean-square (rms) values  $\mu_{XY}$  (planimetry) and  $\mu_Z$  (height) of the theoretical standard deviations of the object point coordinates  $\sigma_x, \sigma_y, \sigma_z$  are calculated. They are computed from the inverted normal equation matrix and the a posteriori reference variance  $\hat{\sigma}_0^2$ . Because the simulations are performed with generated error-free observations, the a priori  $\sigma_0^2$  is used instead of the a posteriori  $\hat{\sigma}_0^2$ . The a priori  $\sigma_0$  is chosen as equal to the standard deviations of the image coordinates. This means, that the accuracy estimates are valid for the a priori assumed precision of the observations.

The presentation and discussion of the results are subdivided in two parts:

- a) the results of the single strip adjustments, assuming normal (bay down) flight attitude of the shuttle (standard flight configurations) and

- b) the results assuming non-standard flight configurations, i. e.
- ▶ 30° cross inclination of the camera carrier or
  - ▶ simultaneous adjustment of two crossing strips with different intersection angles (5°, 30°, 55°).

3.2.1 Standard flight configurations In Figures 4 and 5 the rms values  $\mu_{XY}$  and  $\mu_Z$  of all 3-ray point coordinates are shown graphically with the following abbreviations:

- ▶ 12 km, 23 km, 160 km: distances between orientation images,
- ▶ error-free (0m/0mgrad), 1m/5mgrad, 2m/10mgrad: standard deviations of the position and attitude data (relative accuracy),
- ▶ no observ.: no observations for the position and attitude data,
- ▶ XYZ GCP: 4 error-free XYZ GCP,
- ▶ XY GCP/DTM: 125 XY GCP ( $\sigma=25m$ ) and a DTM ( $\sigma=50 m$ ) as ground control information.

Breaks in the graphic representations mean, that the respective values are not given true to scale.

First, the rms values for the theoretical accuracy limits of the object point coordinates, which are achieved if the exterior orientation parameters of all images are treated as error-free observations, can be seen in the Figures 4 and 5. For 3-ray points these values are:

- a)  $\mu_{XY} = 1.4 m, \mu_Z = 6.1 m$   
for 4 XYZ GCP (error-free);
- b)  $\mu_{XY} = 4.5 m, \mu_Z = 5.1 m$   
for 125 XY GCP ( $\sigma=25m$ ) and DTM ( $\sigma=50m$ ).

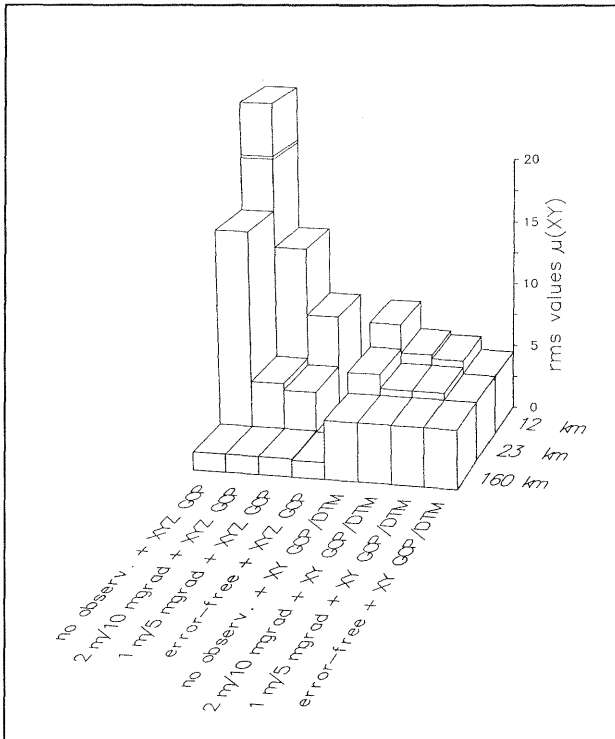


Fig. 4: Rms values  $\mu_{XY}$  for different standard deviations of the exterior orientation parameters, ground control information and distances between orientation images

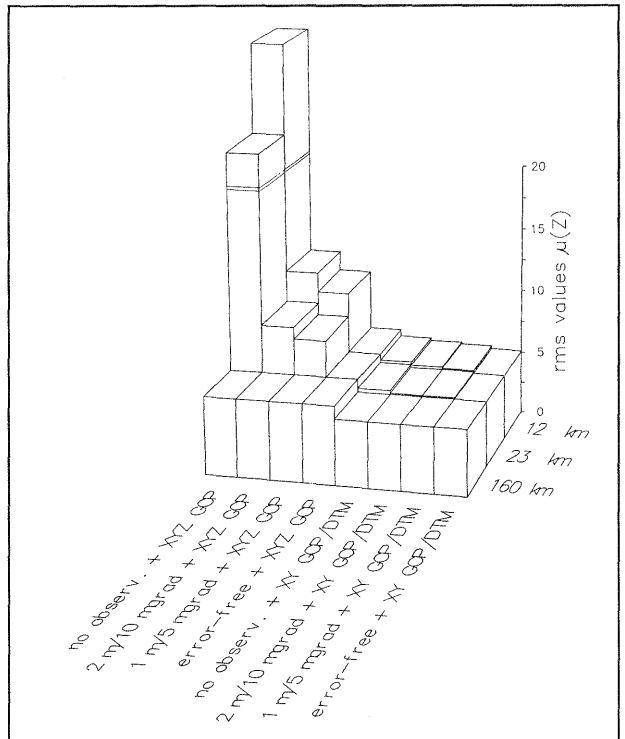


Fig. 5: Rms values  $\mu_Z$  for different standard deviations of the exterior orientation parameters, ground control information and distances between orientation images

$\mu_z$  in a) is estimated poorer by about a factor of 4 than  $\mu_{xy}$ , due to the geometry of the three-line scanner (see chapter 2.1). The planimetric accuracy limit in b) increases by a factor of 3 in comparison with that in a), because the changed control information (125 XY GCP with  $\sigma = 25\text{m}$  instead of error-free GCP) defines the datum in planimetry less accurately. The height accuracy limit in b), however, is improved in comparison with that in a), because the changed control information defines the datum in height more accurately. The DTM namely supplies height control information for all 11.905 object points.

Moreover, the resulting accuracy improves generally with better precision of the position and attitude observations and with an increasing DOI. This effect is more significant using only 4 GCP than a lot of low accurate XY GCP and a DTM. In case of a long distance (160 km) between the orientation images observations for the exterior orientation are dispensable.

From Figure 4 it is evident that the ground control information derived from topographic maps is not sufficient for attaining a high planimetric accuracy of about 1 to 3 m. Therefore, accurate GCP are required.

Figure 5 shows, that the accuracy demands of the mission ( $\sigma_z = 5\text{ m}$ ) can be fulfilled with a short DOI (12 km) and a standard deviation for the position and attitude data of 2 m / 10 mgrad, on condition that a DTM is available. Using the same DOI (12 km) and the same standard deviation for the position and attitude data (2m/10mgrad) the height accuracy decreases to 12.2 m if there are only 4 XYZ GCP instead of the DTM.

3.2.2 Non-standard flight configurations The computations are carried out with a selected set of input parameters only:

- ▶ DOI: 12 km,
- ▶ standard deviations for position and attitude observations: 2 m/ 10 mgrad (relative accuracy),
- ▶ 4 error free XYZ GCP for each strip, located at the corners of the 3-ray areas.

For these assumptions the aspired accuracy of 5 m obviously can not be achieved with standard flight configurations, as described above. However, the results are considerably improved in case of non-standard flight configurations.

Table 2 shows the rms values  $\mu_{xy}$  and  $\mu_z$  of the theoretical standard deviations  $\sigma_x$ ,  $\sigma_y$  and  $\sigma_z$ . The values are calculated separately for 3-ray and 6-ray points. The number n of the corresponding object points gives an idea of the area,

covered by the respective flight configuration (700 points  $\approx 1000\text{ km}^2$ ). For comparison the results, obtained by standard flight configurations, are listed in the first line.

The simulations, assuming 30° cross inclination of the shuttle results in an improved accuracy of the 3-ray points by a factor of 1.7 in height and of 2.8 in planimetry, compared to the normal flight attitude. Best results are obtained by the simultaneous adjustment of two crossing strips. Within the overlapping 6-ray area a constant accuracy level is achieved, which is nearly independent of the intersection angle. This result is of high practical importance. The weak 3-line geometry, caused by the along track parallel perspective, is completely overcome by the block adjustment of two (or more) intersecting strips. According to the figures in Table 2, small intersection angles are more economic, because they lead to larger 6-ray areas and better accuracy in the 3-ray area. The acquisition of MOMS-02 imagery from crossing orbits is planned. Their ground tracks will mainly be located between 20° and 28.5° northern latitude, which will cause small intersection angles.

#### 4. CONCLUSION AND OUTLOOK

The aspired height accuracy of about 5 m can be achieved either by means of DTM information, derived from existing maps, or by the simultaneous adjustment of two (or more) crossing strips within the overlapping area. The intersection angle is of no importance.

The results are generally improved by more accurate observations of the position and attitude parameters and by an increasing distance between orientation images. High planimetric accuracy is only achieved, if precise ground control points, e. g. from GPS measurements, are available. The weak 3-line geometry along track can essentially be supported either by cross inclination of the shuttle or by the simultaneous adjustment of two or more intersecting strips. After the mission it will be possible to prove these findings by the evaluation of practical data.

The three-line concept for the acquisition of digital stereo imagery has been realized in conjunction with some other important projects: MEOSS, MOMS-PRIRODA and HRSC/WAOSS.

MEOSS stands for Monocular (single lens) Electro-Optical Stereo Scanner. It flew successfully onboard an aircraft in the last years and will be payload on an Indian rocket, scheduled for launch in autumn 1992.

number of strips	intersection angle	cross inclination	3-ray area			6-ray area		
			n	$\mu_{xy}$	$\mu_z$	n	$\mu_{xy}$	$\mu_z$
1	-	0°	5951	13.6	12.2	-	-	-
1	-	30°	5038	4.8	7.0	-	-	-
2	5°	0°	1896	1.9	6.3	5307	1.6	4.9
2	30°	0°	9536	2.4	6.5	1803	1.5	4.7
2	55°	0°	11561	3.4	7.8	1097	1.6	4.8

Table 2: Number of object points n and rms values  $\mu_{xy}$  and  $\mu_z$  for non-standard flight configurations, assuming 12km DOI, 2m/10mgrad std.dev. for position and attitude observations, 4 error-free GCP for each strip.

MOMS-PRIRODA is planned as a follow on project of the MOMS-02/D2 mission. The MOMS-02 camera is intended to fly for about three years on the PRIRODA module of the soviet MIR space station. Its orbit inclination of 51.6° allows for acquisition of imagery from industrial countries also.

HRSC (High Resolution Stereo Camera) and WAOSS (Wide Angle Optoelectronic Stereo Scanner) are two of the most promising payloads of the Russian mission to the planet Mars in 1994 (Albertz et al., 1992). From mapping the Red Planet at high resolution in stereo and colour simultaneously new and unique scientific results will be obtained.

## 5. REFERENCES

- Ackermann, F., Bodechtel, J., Lanzl, F., Meissner, D., Seige, P., Winkenbach, H. (1990): "MOMS-02 - A Multispectral Stereo Imager for the Second German Spacelab Mission D2", Int. Arch. of Photogrammetry and Remote Sensing, Vol. 28, Part 1, pp. 110-116.*
- Albertz, J., Ebner, H., Heipke, C., Neukum, G., Scholten, F. (1992): "The Camera Experiments HRSC and WAOSS on the MARS 94 Mission", Int. Arch. of Photogrammetry and Remote Sensing, Vol. 29, Part 1.*
- Aumann, G., Ebner, H. (1992): "Generation of High Fidelity Digital Terrain Models from Contours", Int. Arch. of Photogrammetry and Remote Sensing, Vol. 29, Part 1.*
- Ebner, H., Hofmann, O., Kornus, W., Müller, F., Strunz, G. (1991): "A Simulation Study on Point Determination Using MOMS-02/D2 Imagery", Photogrammetric Engineering & Remote Sensing, Vol. 57, No. 10, pp. 1315-1320.*
- Ebner, H., Kornus, W. (1991): "Point Determination Using MOMS-02/D2 Imagery". Conference Proceedings IGARSS, Helsinki 1991, Vol. III, pp. 1743-1746.*
- Ebner, H., Müller, F., Zhang, S. (1988): "Studies on Object Reconstruction from Space Using Digital Data of Three Line Scanner Imagery", Int. Arch. of Photogrammetry and Remote Sensing, Vol. 27, Part B11, pp. I/242-I/249.*
- Ebner, H., Strunz, G. (1988): "Combined Point Determination Using Digital Terrain Models as Control Information", Int. Arch. of Photogrammetry and Remote Sensing, Vol. 27, Part B11, pp. III/578-587.*
- Heipke, C., Kornus, W., Gill, R., Lehner, M. (1990): "Mapping Technology Based on 3-Line-Camera Imagery", Int. Arch. of Photogrammetry and Remote Sensing, Vol. 28/4, pp. 314-323.*
- Müller, F. (1991): "Photogrammetrische Punktbestimmung mit Bilddaten digitaler Dreizeilenkameras", Deutsche Geodätische Kommission, Reihe C, Heft Nr. 372, München.*
- Technical University Munich (1992): "CLIC - Bundle Block Adjustment Program", Product Information and User's Manual.*
- Wu, J. (1986): "Geometrische Analyse für Bilddaten stereoskopischer Dreifach-Linearzeilenabtaster", Wiss. Arbeiten der Fachrichtung Vermessungswesen der Univ. Hannover, Heft Nr. 146.*